RSC Advances

RSC Advances

www.rsc.org/advances

ROYAL SOCIETY OF CHEMISTRY

www.rsc.org/advances

Graphical Abstract:

A facile method was reported to generate monodispersed QD coded alginate microbeads by employing a simple microfluidic device using internal gelation approach. The application of the as-prepared microbeads for suspension assay was demonstrated.
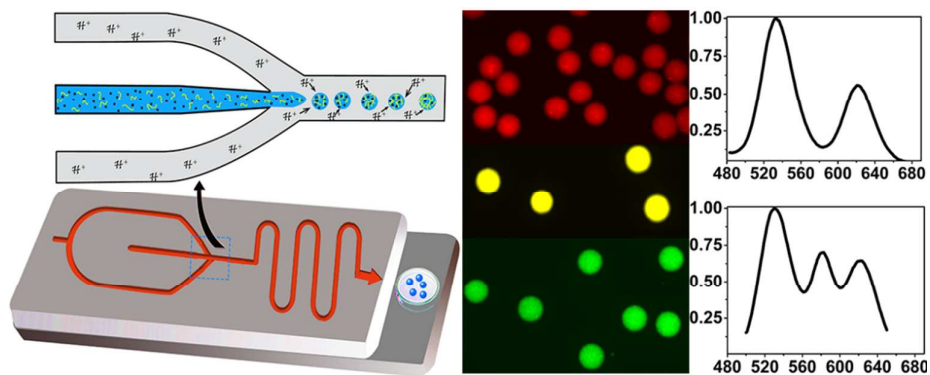
Journal Name

ARTICLE

Microfluidic Generation of Uniform Quantum Dot-encoded Microbeads by Gelation of Alginate

Huan Liu[a,b], Guohua Li[a,b], Xiangyu Sun[a,b], Yonghong He[a,b], Shuqing Sun[a,b]*, Hui Ma[a,b]

We report a very facile microfluidic strategy for the fabrication of monodispersed fluorescent quantum dot (QD)-embedded alginate barcodes. In this work, nano-sized calcium carbonate ($CaCO_3$) is added to the dispersed phase and used as the crosslinking anent for internal gelation of alginate. The as-prepared microspheres exhibit uniform size distribution (CV=2.7%). By tuning the quantity of the quantum dots with different emission wavelengthes added to the dispersed phase, single color and multiple color barcode particles are successfully prepared in a flow focusing microfluidic devices, which may be useful for various applications.

Introduction

Multiplex suspension array assay has been widely used in clinical diagnostic, drug discovery, bioimaging and so on,[1] in which the technology need simultaneously analyze multiple species in a single assay. Compared with the conventional solid-phase biochips, barcode microbeads in suspension arrays have been emerging as attractive approaches for multiplexed detection of biomolecules. The advantages of using a microbead-encoding strategy include enhanced conjugation of analyte (more effective capture of analytes), shorter incubation time, more cost effective and higher sensitivity.[1b,2] Especially, with the development of the flow cytometry technology, the detection speed of suspension array had achieved to 10000 barcodes per second that enables multiplex analysis possible.[3] Several coding scheme have been developed, mainly including spectroscopic barcodes, graphical barcodes and Raman spectral barcodes.[4] Among the encoding strategies explored, spectroscopic encoding is the most well-established scheme. Fluorescent barcoded particles can be easily readout by using a flow cytometry system.[5]

However, how to effectively prepare coding microspheres is still a bottleneck for suspension array technology. The monodispersed coding beads are used as the reaction carrier with the following requirements: a regular spherical structure, a narrow size-distributed region and containing steady and precise fluorescent coding signals. The polystyrene (PS) beads doped with organic fluorescent dye have been a commercial product, but the organic dyes easily suffer fluorescence

quenching and need different excitation light sources for exciting various dyes. In order to meet the detection requirement of high-throughput and high-sensitivity, quantum dots (QDs) encoded microbeads have become an attractive option owing to the unique properties of QDs including narrow photoluminescence (PL) emission spectrum, high quantum yield and good photostability. In particular, a single wavelength can be used for simultaneous excitation of all different-sized QDs which allow the possibility for practice application,[6] which greatly reduces the complexity and cost of instrumentation.

Strategies that are commonly used for the preparation of QD barcodes include the "swelling" technique,[6a,7] QD entrapment inside layer-by-layer charged polymer coatings[8] and polymerizable QD encapsulation.[9] However, these approaches present many significant disadvantages, namely, QDs leak from the bead, the process is tedious and lengthy, and fluorescence intensity isn't stable when exposed to various pH values.[10] These problems have limited the applications of QD encoded particles. Microfluidics is an effective approach to overcome these problems and offers high flexibility, productivity, and good repeatability.[11] Especially, it is easy to achieve any composition of QD in the microbeads by simply adding them into dispersion phase prior to injection. In addition, microfluidics can generate monodisperse particles with precise control over the size, shape and composition by changing the flow rates of the two immiscible phases and geometries of microfluidic devices.[12]

Alginate is a linear copolymer composed β-D-mannuronic acid and α-L-guluronic acid,[13] it can easily form hydrogels when meets with multivalent cations such as Ca^{2+}, Ba^{2+} and so on. Gelation strategies mainly involve external and internal source of crosslinking agent to polymerize alginate droplets generated by microfluidic, which have important influence on getting highly uniform barcodes. For external gelation, the

a. Institute of optical imaging and sensing, Shenzhen Key Laboratory for Minimal Invasive Medical Technologies, Graduate School at Shenzhen, Tsinghua University, Shenzhen 518055, China
b. Department of Physics, Tsinghua University, Beijing 100084, China
* To whom correspondence should be addressed. Email: sun.shuqing@sz.tsinghua.edu.cn

droplets first formed in microfluidic device and then the alginate on the bead surface crossed linked upon meeting with divalent ion in solution. The resulted microbeads usually exhibit non-spherical morphology carrying a tail due to the rapid gelation rate.[14] The other alternative, internal gelation, an inactive crosslinking agent was added to the disperse phase and upon injection into the continuous phase, an activation agent diffuse into the formed droplets to activate and release the crosslinking agent. [15] The surface of an alginate microbead bears abundant carboxylic groups, which enables its hydrophilic character and allows easy conjugation with DNA or proteins. Alginate hydrogels are inherently nontoxic and biodegradable, and have also been used for cell encapsulation and drug delivery etc..[16]

In this study, we present the use of $CaCO_3$ nanoparticles as crosslinking agent to produce QD-tagged barcodes in a microfluidic device by internal gelation. The obtained barcodes show very narrow size distribution and good spherical structure, and exhibit uniform spectral characteristics and excellent encoding capability. In addition, this synthesis method is extremely facile and avoids complicated gelation steps. These features enable the barcode microbeads an ideal candidate for biomedical applications.

Experimental

Materials

Alginic acid sodium salt from brown algae, rabbit IgG (1 mg/mL) and calcium chloride were purchased from Sigma-Aldrich. N-hexadecane (99%) was purchased from Alfa. Acetic acid glacial and n-Hexane were obtained from Tianjin Zhiyuan Chemical Reagent Co. Ltd. (China), the surfactants EM 90 was obtained from ABIL. Calcium carbonate ($CaCO_3$) (40 nm) was kindly provided by Nano-Materials Technology Pte Ltd. (Singapore). Tween 20 was purchased from Tianjin Fuchen Chemical Reagents Factory (China). Aqueous CdSe/ZnS QDs (8.0 µM) modified by mercaptoacetic acid with emission peak with 525, 580, 595 and 625 nm were obtained from Wuhan Jiayuan Quantum Dots Co. Ltd. (China). Aqueous CdTe QDs (5.0 µM, 670 nm) with carboxyl were purchased from Beijing Beida Jubang Science & Technology Co. Ltd. (China). FITC-labeled goat anti-rabbit IgG (0.5 mg/ml) was purchased from Southern Biotech (USA). The deionized water was obtained from Millipore Milli-Q water purification with a specific resistance of 18 MΩ cm. All materials were used as procured received without further purification.

Microfluidic Devices

The microfluidic chip was fabricated by photolithography. Namely, a mold of the microfluidic network was made on a piece of silicon wafer by photolithography of SU8-2015 photoresists. Then the microfluidic network was replicated from silicon wafer to polydimethylsiloxane (PDMS，RTV615, Momentive, USA). The resulting PDMS replica was bonded to 25 mm by 75 mm glass substrate following oxygen plasma treatment of both surfaces.

Preparation of the Quantum Dot Embedded Microbeads

The disperse phase was the hydrophilic alginate aqueous solution containing various concentrations of above QDs with different emission wavelengths. Disperse and continuous fluids were introduced into the microfluidic device through polytetrafluoroethylene tubing, and the flow rates were controlled using two syringe pumps (Pump 11 Elite, Harvard Apparatus; LSP01-1A, Baoding Longer Precision Pump Co.) and gastight syringes (SGE). Under these optimal conditions, emulsion droplets can be fabricated by adjusting the flow rates, and monodispersed QDs-embedded microbeads can be produced by in-situ internal gelation.

QD-encoded beads-based immunoassays

First, about fifty thousand QD-encoded microspheres were employed to attach antigen rabbit IgG in 100 µL of PBS (0.01 M, pH 7.4) for 1 h and were washed with PBS three times. Next, the microspheres were suspended in 1 wt% BSA at room temperature for 2h to reduce nonspecific interactions. For the immunofluorescence, both the experimental group and control group were carried out in the same manner with rabbit IgG and BSA. Finally, 50 µL FITC-labeled goat anti-rabbit IgG were added into the suspension and mixed for 1h and the particles were washed with PBS for three times. The resulted solution was stored in 200 µL PBS for flow cytometer detection.

Characterization

The optical micrograph of the microbeads were captured by CCD camera mounted on an inverted microscope the microscope (Olympus IX2-UCB). A fluorescence microscope (Olympus) was used to acquire images of the fluorescent beads. The fluorescence spectrums of QD-encoded microbeads were analyzed by a spectrofluorophotometer (RF-5301PC, SHIMADZU). The structure of the QD-doped barcode were examined by a laser scanning confocal microscope (LSCM, FV1000, Olympus) to characterize the distribution of QD inside a microbead. The average droplet size and the coefficient of variation (CV) were determined by measuring the sizes of at least 160 particles in an image using software (Image-Pro Plus) and the coefficient of variation (CV) is defined by the following equation CV = δ/d_{av} ×100%, where δ is the standard deviation, and d_{av} is the average droplet diameter.

A flow cytometer (FACS Calibur, BD) was used to analyze the suspension immunoassays. QD-encoded beads in PBS solution were injected into the flow cytometer. Signals from 10,000 microspheres were collected for each sample and were excited by a 488 nm laser.

Results and discussion

A flow focusing microfluidic device are utilized to fabricate alginate microspheres, compared to T-junction design, the flow focusing system improves the stability of fluid in channel and prevents the dispersed phase contacting with channel walls to corrode the channel.[17] The microfluidic microbead generation device consists of two parts: a nozzle zone for the

breakup of barcode droplets and a snakelike zone used to solidify the microbeads by in situ gelation that can ensure the monodispersity of the microbeads. In the nozzle zone (Figure 1a), the dispersed phase consisting of alginate solution, nano-sized $CaCO_3$ and QDs, was connected to the microfluidic device from inlet A using a syringe pump, and biocompatible microparticles were constructed by shearing the disperse phase alginate aqueous solution mixed with different QDs into microdroplets by two steady continuous phase (hexadecane and acetic acid) injected from inlet B. Because internal gelation requires plenty residence time for sufficient crosslinking, an S-shaped channel with gradually increasing width are designed in order to possess abundant reaction time for gelation and prevent coalescence. Figure 1b shows the CAD design drawing of microfluidic channel. Figure 1c is the photograph of the microfluidic device.

Gelation of alginate droplets is of importance to obtain size-controlled and well-defined encoding microspheres. For external gelation, the droplets formed in microfluidic device
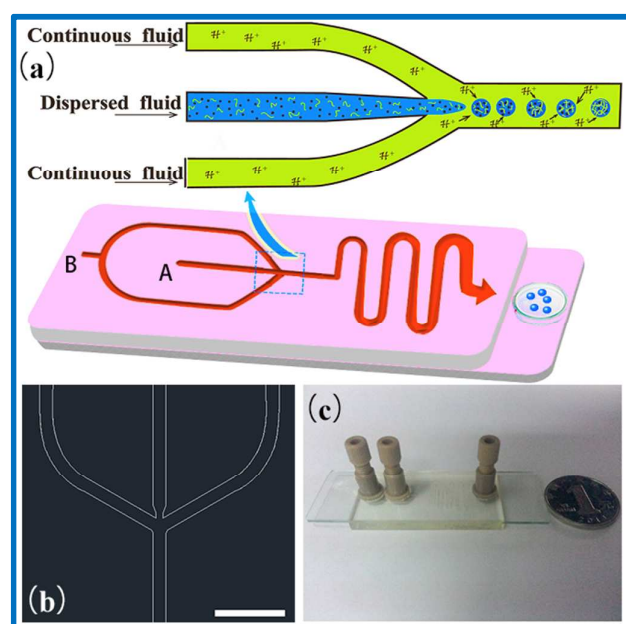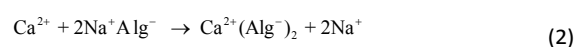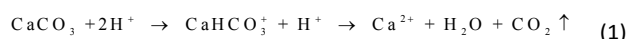

Figure 1. The schematic picture of the designed device and photograph of a microfluidic device fabricated. (a) Schematic diagram of the microfluidic generation of alginate microbeads by the internal on-line gelation. Nano-sized $CaCO_3$ is added into the disperse phase as crosslinking agent and introduced in the center channel. Acetic acid in continuous fluid creating an acidic environment for releasing Ca^{2+} is supplied to the side channels. In the gelation process, H^+ diffuses into the aqueous droplets to increase the dissolution of $CaCO_3$ and subsequently Ca^{2+} ionically crosslink alginate. The alginate droplets complete crosslinking reaction in the snakelike channels. (b) The CAD drawing of Schematic of the nozzle zone with 40×100 μm nozzle in the center for ejecting alginate aqueous solution. Hexadecane is introduced through the cross channels with 70×100 μm (scale bar = 300 um). (c) The photograph of fabricated PDMS droplet device.

are transferred into an aqueous solution of a crosslinking agent such as $CaCl_2$, this gelation process is always requiring a long time to ensure a completely crosslinking. In the meantime, the off-line of external gelation may lead to the formation of polydisperse alginate microspheres.[18,19] In this experiment, internal gelation was employed by adding nano-sized $CaCO_3$ (about 40 nm) into the dispersed phase as the inactive crosslinking agent and mixing acetic acid with continuous phase. The flow diagram of the experiments and the microfluidic device to generate QD-doped alginate microbeads are shown in Figure 1a. Upon formation of the microspheres, the acetic acid diffuses into the droplets followed by the release of Ca^{2+} (Equation 1). Subsequently Ca^{2+} ions coordinate to the residues of α-L-guluronic acid of alginate resulting in polymer gelation (Equation 2).

$$CaCO_3 + 2H^+ \rightarrow CaHCO_3^+ + H^+ \rightarrow Ca^{2+} + H_2O + CO_2 \uparrow \quad (1)$$

$$Ca^{2+} + 2Na^+Alg^- \rightarrow Ca^{2+}(Alg^-)_2 + 2Na^+ \quad (2)$$

This approach allows the formation of monodispersed barcodes. Meanwhile, the presence of carboxyl groups on the surface of alginate microspheres enable them to be applied for suspension array detection.

As shown in Figure 2, the as-prepared microbeads exhibit good sphericity and fine monodisperisity under an optical microscope. Figure 2c shows that the diameter of alginate microbeads is about 46 μm when the flowing rate of dispersed phase (Q_d) and the continuous phase (Q_c) are 1 μL/min and 30 μL/min, respectively. The coefficient of variation is approximately 2.7%, indicating the narrow size distribution of

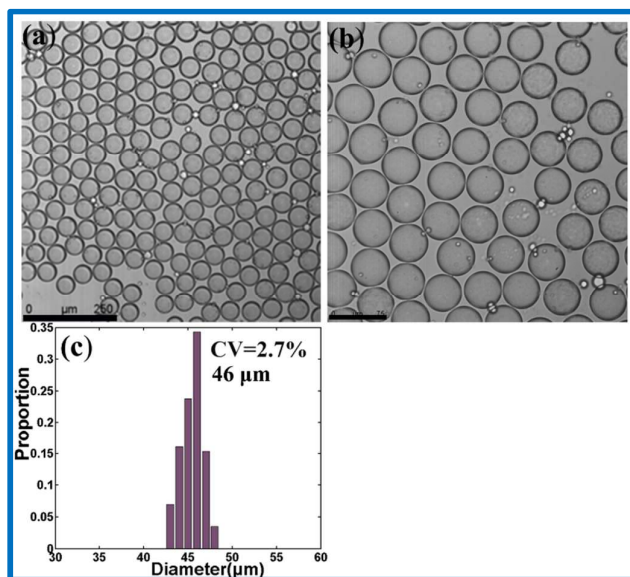Figure 2. (a) Optical microscopy image of alginate microbeads when Q_c=30 μL/min, Q_d=1 μL/min. The scale bar is 250 μm. (b) A higher magnification optical image under the same condition. The scale bar is 75 μm. (c) Size distribution of the microbeads shown in (a) and (b). The mean diameter is 46 μm and the CV is 2.7%.

the resulted microbeads. In addition, this strategy allows rapid production of barcodes particles and about 2.22×10^{4} spheres are generated per minute. The above features indicate it possible to precisely control the contents of QDs in each particle and therefore every bead carries the same optical coding signals under the same preparation parameters.

Figure 3 shows that QDs are encapsulated in alginate microbeads and all particles show bright color of green, yellow and red. To further investigate their optical property, the normalized fluorescent spectra are shown in Figure 3d, in which the solid lines and dotted lines represent fluorescent spectroscopy of QD-encoded microspheres and primary QDs dispersed in deionized water, respectively. Beads loaded with QD-580 nm and QD-625 nm show identical optical characteristics to the loading QDs. Although the emission maximum of QD-525 nm slightly red shifted in microspheres, it doesn't show any adverse effect on subsequent multiple coding.
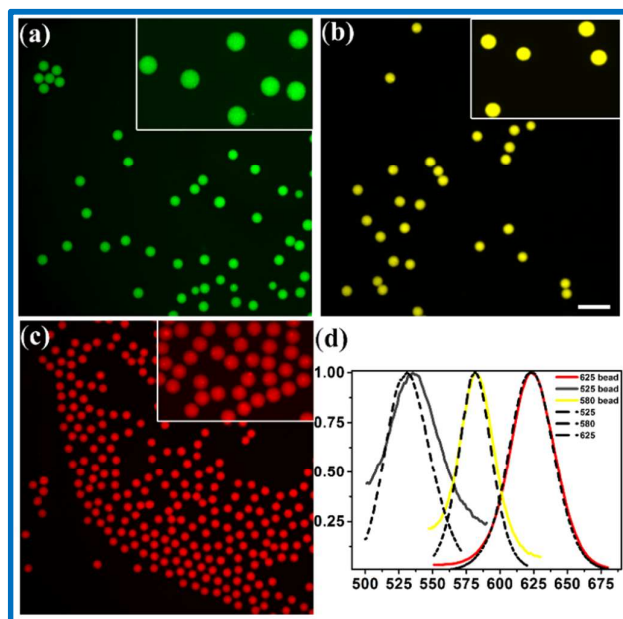

Figure 3. (a), (b) and (c) show the fluorescence microscope image of barcodes doped QD-525 nm, QD-580 nm and QD-625 nm, the insets show enlarged image. (d) The solid lines represent the spectrums of the single color barcodes according to (a), (b) and (c). The dotted lines show the spectrum of original QDs diluting in water. The scale bar is 250 μm.

As shown in Figure 4, the LSCM images, recorded at ten focalized planes from the top to the bottom with the step of 4 μm, reveal that QDs are distributed homogeneously inside the entire sphere. It is evident that QDs have been trapped in the microspheres. We estimate the solid contents of the QDs trapped in beads could reach 4.6 wt. %, which shows a high QD loading and concentration-controlled ability in the microfluidic approach.
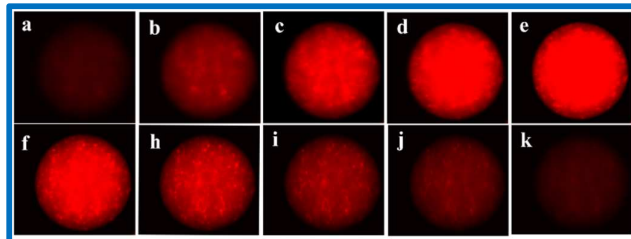

Figure 4. Confocal fluorescence microscopy images of alginate bead generated by doping the QD-625 nm at different focalized planes from the top to the bottom of one bead, and the step size is 4 μm.

For multicolor encoding, the fluorescence intensities of QD-doped barcodes are proportional to the molar concentration of QDs in disperse phase, namely the higher concentration and the higher fluorescent intensity. This principle offers the possibility to create a huge number of barcodes through simply mixing different concentrations and wavelengths QDs with alginate aqueous solution. To further demonstrate this approach, we employed two out of four colored QDs combined with three intensity levels to obtain ten unique barcodes. Considering the spectral overlap, two combinations were selected to get distinguished coding spectrum, in which 525nm and 625nm QDs were combined in a group and the same for 595nm and 670nm QDs. As showed in Figure 5, every color QD was set as three light intensities, namely 1, 2 and 4. By simply adjusting the QDs concentration in dispersed phase, the barcode of 1:4, 1:2, 2:1, 4:1 and 1:1 were successfully prepared by using the pair-QDs combination according to 595 nm:670 nm and 525 nm:625 nm. The resulted barcodes don't exhibit spectral overlap and fluorescence resonance energy transfer phenomena, but carry a series of controlled encoded signals.

In addition, three color QDs were selected for encoding, and coding signals of 1:2:4, 1:2:1, 1:1:1 and 2:1:1 were obtained, as shown in Figure 6a, 6b, 6c and 6d, respectively. Simultaneously, in Figure 6a, the spectrum of original QDs are compared with that of the encoded beads, in which the green, blue and red dotted lines correspond to the QD-525 nm, QD-580 nm and QD-625 nm emission line, respectively. The 525 nm and 580 nm QDs are lightly red shifted but Förster resonance energy transfer (FRET) is not observed. In spite of the appearance of some spectral overlapping, the final barcodes still show unique and recognized signatures. Thus this strategy provides a facile way to the generation of high quality fluorescent barcoded microbeads for multiplexed sensing applications.
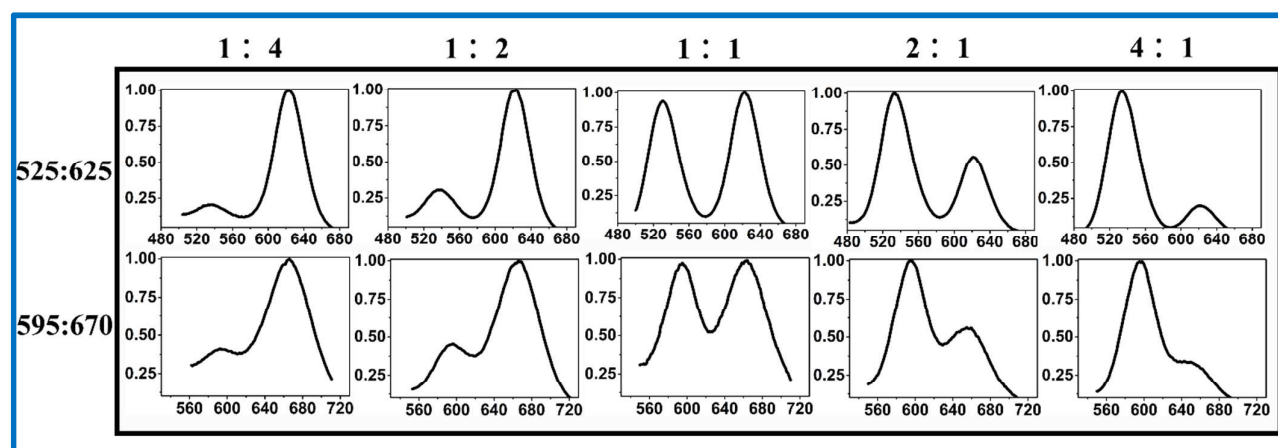
Figure 5. Representative spectra of QDs-encoded beads containing two types of QDs 525:625 nm and 595:670 nm to create 1:4, 1:2, 1:1, 2:1 and 4:1 coding signals.
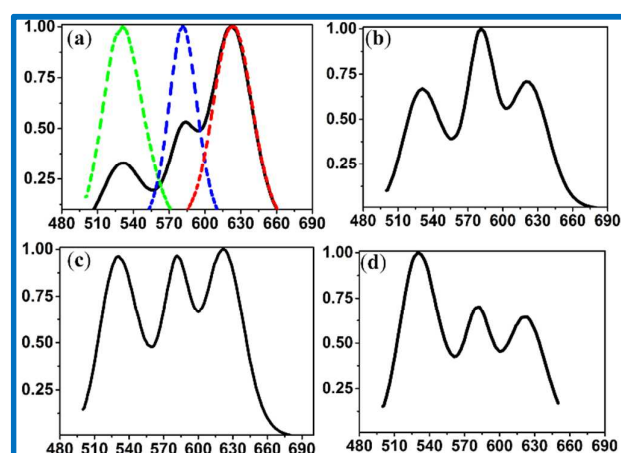

Figure 6. Typical spectra of tricolor QD-tagged microbeads encoding by 525 nm, 580 nm and 625 nm.

Flow cytometry is an effective technique for decoding the QD-encoded barcodes, which can detect both size and spectroscopic signals. In Figure 7a, two-dimension scatter diagram indicates that the microspheres have a uniform size distribution. Another scatter plot was obtained (Figure 7b) for barcodes carrying two color QDs, in which QD-525 nm and QD-625 nm were analyzed by detection channels of FL1 and FL3, respectively. And the four dots represented the signals from two QD-encoded microspheres and this stated that the resulted barcodes could be applied for multiplexed detection.
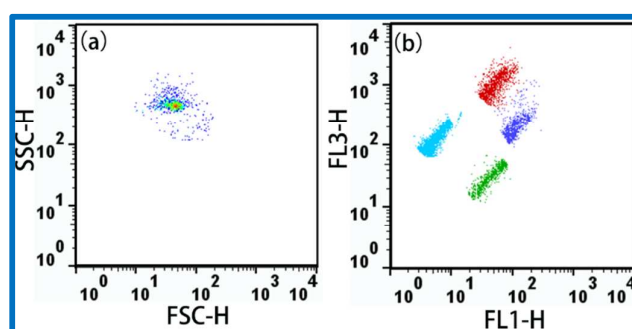

Figure 7. The flow cytometer analysis diagrams of QD-encoded alginate beads. (a) The bead populations based on side light scatter (SS) vs. forward light scatter (FS). (b) Plot of FL4 versus FL1 for the QD-encoded fluorescent barcodes.

In order to demonstrate the applicability of QD-encoded alginate beads in biological assays, a simple immunoassay was carried out using QD-625nm-encoded beads. The rabbit IgG were immobilized on the surface of QD-encoded beads by a non-covalent adsorption method[20], and the antigen-immobilized particles were used to detect the FITC-labeled goat anti-rabbit IgG (shown in Figure 8a). The fluorescence signals of FITC and QD-625 nm were measured by FL1 and FL3 channels, respectively. And all samples on FL3 channel are constant. Figure 7b shows that the fluorescence intensities in FL1 channel between BSA control group (b1, b3) and FITC group (b2, b4) are obviously different, in which the intensity of FITC group is higher than the BSA group. So these fluorescent microspheres can offer much promise for multiplexed assay in the future.
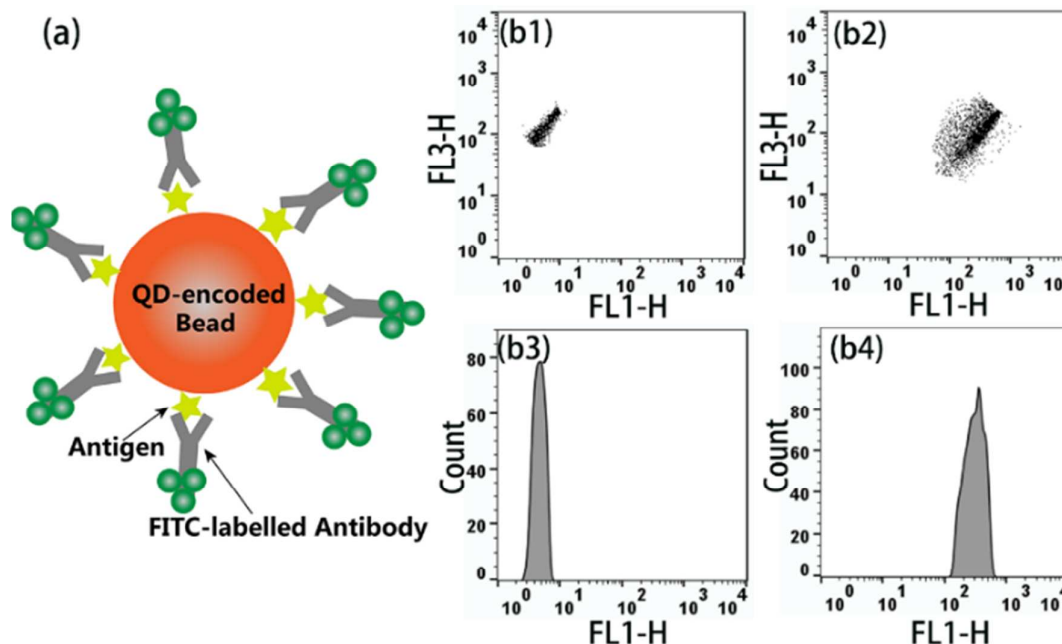
Figure 8. (a) Schematic diagram of the immunoreactions. (b) The flow cytometer analysis of QD-encoded bead-based immunoassays for BSA control group (b1 and b3) and FITC group (b2 and b4). Here the emission wavelength of QD-encoded microspheres is 625 nm which can be measured on the FL3 channel for decoding of encoded beads, and the fluorescent intensities of all samples on FL3 channel are constant. The FITC fluorescence signal was measured on the FL1 channel for the decoding of FITC-labeled goat anti-rabbit IgG antibody.

Conclusions

In conclusion, we designed a simple flow focusing PDMS microfluidic device for the generation of alginate microparticles, which features an S-shaped channel with gradually increased width to guarantee sufficient reaction time for gelation and to avoid coalescence and clogging issues. The alginate droplets performed crosslinking reaction by internal in-situ gelation using nano-sized $CaCO_3$, and the monodispersed microbeads with the diameter of 46 μm were generated on a large scale (CV=2.7%). It is demonstrated that QDs were evenly distributed in the microspheres in a QD-encoded alginate beads, and the fluorescence performance of the QDs is well reserved without significant peak broadening or distortion, which enabling those microspheres a promising candidate for optical encoding. The use of various QD combinations of two or three for multiple encoding process are also performed, and it demonstrates that the microbeads can be encoded with different QDs as well as intensity ratio of fluorescence at different wavelengths. We envisage those fluorescent microspheres could find wide application in the field of multiplexed sensing system.

Acknowledgements

References

1   a) K. Braeckmans, S. C. De Smedt, C. Roelant, M. Leblans, R. Pauwels, J. Demeester, *Nat. Mater.,* 2003, **2**, 169; b) R. Wilson, A. R. Cossins, D. G. Spiller, *Angew*. *Chem. Int. Ed.,* 2006, **45**, 6104; c) X. H. Gao, Y. Y. Cui, R. M. Levenson, L. W. K. Chung, S. M. Nie, *Nat. Biotechnol*., 2004, **22**, 969; d) J. K. Jaiswal, H. Mattoussi, J. M. Mauro, S. M. Simon, *Nat. Biotechnol*., 2003, **21**, 47.

2   T. R. Sathe, A. Agrawal, S. M. Nie, *Anal. Chem*., 2006, **78**, 5627.

3   a) G. Wang, Y. K. Leng, H. J. Dou, L. Wang, W. W. Li, X. B. Wang, K. Sun, L. S. Shen, X. L. Yuan, J. Y. Li, K. Sun, J. S. Han, H. S Xiao, Y. Li, *ACS. Nano*., 2012, **7**, 471; b) G. Wang, Y. K. Leng, H. Z. Guo, S. Song, Z. Q. Jiang, X.L. Yuan, X. B. Wang, K. Sun, K. Sun, H. G. Dou, *J. Mater. Chem. B.,* 2014, **2**, 8310.

4   a) N. H. Finkel, X. H. Lou, C. Y. Wang, L. He, *Anal. Chem*., 2004, **76**, 353; b) Y.J. Zhao, Y. Cheng, L.R. Shang, J. Wang, Z.Y. Xie, Z. Z. Gu, *Small*, 2015, **11**, 151; c) Y. M. Lai, S. Q. Sun, T. He, S. Schlucker, Y. L. Wang, *RSC Adv*., 2015, **5**, 13762.

5   a) S. R. Nicewarner-Pena, R. G. Freeman, B. D. Reiss, L. He, D. J. Pena, I. D. Walton, R. Cromer, C. D. Keating, M. J. Natan, *Science*, 2001, **294**, 137; b) M. S. Gudiksen, L. J. Lauhon, J. Wang, D. C. Smith, C. M. Lieber, *Nature*, 2002, **415**, 617.

6   a) M. Y. Han, X. H. Gao, J. Z. Su, S. M. Nie, *Nat. Biotechnol*., 2001, **19**, 631; b) U. Resch-Genger, M. Grabolle, S. Cavaliere-

Jaricot, R. Nitschke, T. Nann, *Nat. Methods*, 2008, **5**, 763; c) J. Wang, Y. X. Liu, F. Peng, C. Y. Chen, Y. H. He, H. Ma, L. X. Cao, S. Q. Sun, *Small*, 2012, **8**, 2430; d) F. Li, J. Wang, S. Q. Sun, H. Wang, Z. Y. Tang, G. J. Nie, *Small*, 2015, **11**, 1954.

7   T. Song, Q. Zhang, C. L. Lu, X. Q. Gong, Q. H. Yang, Y. H. Li, J. Q. Liu,, J. Chang, *J. Mater. Chem*., 2011, **21**, 2169.

8   a) S. Rauf, A. Glidle, J. M. Cooper, *Adv. Mater*., 2009, **21**, 4020; b) J. Li, X. W. Zhao, Y. J. Zhao, J. Hu, M. Xu, Z. Z. Gu, *J. Mater. Chem*., 2009, **19**, 6492.

9   W. C. Sheng, S. Kim, J. Lee, S. W. Kim, K. Jensen, M. G. Bawendi, *Langmuir*, 2006, **22**, 3782.

10   J. A. Lee, A. Hung, S. Mardyani, A. Rhee, J. Klostranec, Y. Mu, D. Li, W. C.W. Chan, *Adv. Mater*., 2007, **19**, 3113.

11   a) S.-K. Lee, J. Baek, K.F. Jensen, *Langmuir*, 2014, **30**, 2216; b) K. Q. Jiang, C. Xue, C. D. Arya, C. R. Shao, E. O. George, D. L. DeVoe, S. R. Raghavan, *Small*, 2011, **7**, 2470; c) I. Lee, Y. Yoo, Z. D. Cheng, H. K. Jeong, *Adv. Funct. Mater*., 2008, **18**, 4014; d) Y. J. Zhao, H. C. Shum, H. S. Chen, L. L. A. Adams, Z. Z. Gu, D. A. Weitz, *J. Am. Chem. Soc*., 2011, **133**, 8790.

12   a) S. Fournier-Bidoz, T. L. Jennings, J. M. Klostranec, W. Fung, A. Rhee, D. Li, W. C. W. Chan, *Angew. Chem. Int. Ed*., 2008, **47**, 5577; b) Y. Chen, P. F. Dong, J. H. Xu, G. S. Luo, *Langmuir*, 2014, **30**, 8538; c) C. H. Yang, K. S. Huang, Y. S. Lin, K. Lu, C. C. Tzeng, E. C. Wang, C. H. Lin, W.Y. Hsu, J. Y. Chang, *Lab Chip*, 2009, **9**, 961; d) K. Xu, X. H. Ge, J. P. Huang, Z. X. Dang, J. H. Xu, G. S. Luo, *RSC Adv.,* 2015, **5**, 46981; e) T. Ono, M. Yamada, Y. Suzuki, T. Taniguchi, M. Seki, *RSC Adv*., 2014, **4**, 13557.

13   L. Capretto, S. Mazzitelli, C. Balestra, A. Tosib, C. Nastruzzi, *Lab Chip*, 2008, **8**, 617.

14   H. Zhang, E. Tumarkin, R. Peerani, Z. Nie, R. M. A. Sullan, G. C. Walker, E. Kumacheva, *J. Am. Chem. Soc*., 2006, **128**, 12205.

15   W. H. Tan, S. Takeuchi, *Adv. Mater*., 2007, **19**, 2696.

16   a) C. H. Choi, J. H. Jung, Y. W. Rhee, D. P. Kim, S. E. Shim, C. S. Lee, *Biomed Microdevices*, 2007, **9**, 855; b) S. Akbari, T. Pirbodaghi, *Microfluid Nanofluid*, 2014, **16**,773; c) H. Onoe, K. Inamori, M. Takinouec, S. Takeuchi, *RSC Adv*., 2014, **4**, 30480.

17   a) J. H. Xu, S. W. Li, J. Tan, G. S. Luo, *Microfluid Nanofluid*, 2008, **5**, 711; b) K. S. Huang, Y. S. Lin, C. H. Yang, C. W. Tsaid, M. Y. Hsu, *Soft Matter*, 2011, **7**, 6713.

18   A. Fang, B. Cathala, *Colloids Surf. B: Biointerfaces*, 2011, **82**, 81.

19   X. H. Ji, W. Cheng, F. Guo, W Liu, S. S. Guo, Z. K. He, X. Z. Zhao, *Lab Chip*, 2011, **11**, 2561.

20   W. Y. Yuan, H. Dong, C. M. Li, X. Q. Cui, L. Yu, Z. S. Lu, Q. Zhou, *Langmuir*, 2007, **23**, 13046.